SCIENTIFIC REPORTS

OPEN

SUBJECT AREAS:
DENDRIMERS
POLYMER CHEMISTRY
NANOSCIENCE AND TECHNOLOGY
COORDINATION CHEMISTRY

Received
12 March 2013

Accepted
21 May 2013

Published
7 June 2013

Correspondence and requests for materials should be addressed to N.S. (SATOH.Norifusa@nims.go.jp) or K.Y. (yamamoto@res.titech.ac.jp)

Metastability of anatase: size dependent and irreversible anatase-rutile phase transition in atomic-level precise titania

Norifusa Satoh[1], Toshio Nakashima[2] & Kimihisa Yamamoto[2]

[1]Photovoltaic Materials Unit, National Institute for Materials Science, 1-2-1 Sengen, Tsukuba, Ibaraki, 305-0047 Japan, [2]Chemical Resources Laboratory, Tokyo Institute of Technology, 4259 Nagatsuta, Yokohama 226-8503 Japan.

Since crystal phase dominantly affects the properties of nanocrystals, phase control is important for the applications. To demonstrate the size dependence in anatase-rutile phase transition of titania, we used quantum-size titania prepared from the restricted number of titanium ions within dendrimer templates for size precision purposes and optical wave guide spectroscopy for the detection. Contrary to some theoretical calculations, the observed irreversibility in the transition indicates the metastablity of anatase; thermodynamics cannot explain the formation of metastable states. Therefore, we take into account the kinetic control polymerization of TiO_6 octahedral units to explain how the crystal phase of the crystal-nucleus-size titania is dependent on which coordination sites, *cis*- or *trans*-, react in the TiO_6 octahedra, suggesting possibilities for the synthetic phase control of nanocrystals. In short, the dendrimer templates give access to crystal nucleation chemistry. The paper will also contribute to the creation of artificial metastable nanostructures with atomic-level precision.

The size dependence of nanocrystals during a solid-solid phase transition has attracted much attention[1,2], because phase control is a key step to improve functionalities in photovoltaics[3,4], ferroelectricity[5], magnetics[6], and oxygen permeability[7] for various applications, such as solar cells, memories, and fuel cells. In terms of the melting point of nanocrystals, the thermal behaviours of nanocrystals have an inverse size dependence in the phase transition temperature due to the direct correlation to the volume and surface ratio[8–13]. However, irreversible solid-solid phase transitions from metastable states to the stable states cannot define any specific transition temperature based on thermodynamics due to the absence of any phase equilibrium. Therefore, the discussions on melting point can primarily apply to reversible solid-solid phase transitions at the equilibrium state, but not for irreversible transitions. Similarly, it is also not possible to define any phase diagram for irreversible phase transitions. During the irreversible transitions, however, the atoms obtain freedom in motion from the metastable phase structure and then irreversibly transform into the most stable phase structure. Based on the similarity between melting and the initiation of the transition process, we presume that the transition initiation temperature for the irreversible process is the temperature at which the atoms start moving freely toward the thermal stable states as the phase transition through the melting-like process. For the above-mentioned conditions, we can hypothesize the transition initiation temperature depending on size in a similar manner to melting as follows:

$$T(r) \approx T_{\mathrm{bulk}} - \frac{A}{r} \tag{1}$$

where r is radius of nanocrystals, $T(r)$ is size-dependent transition initiation temperature, T_{bulk} is the transition initiation temperature in bulk, and A is a constant. The transition initiation temperature for irreversible solid-solid phase transitions also decreases inversely with the size.

Although nano-size titania (TiO_2), an attractive material for photocatalysts, dye-sensitized solar cells (DSCs), and organic thin film solar cells[14–16], has shown irreversible anatase-rutile phase transition at low temperature, a clear size dependence has not yet been observed in the transition initiation temperature. The phase control of anatase or rutile is also important in these performances due to the different band diagram and surface chemical activities. Thus, many researches have attempted to reveal the influences on the thermal phase transition from anatase to rutile caused by impurities[17], heat conditions[18,19], and the sample preparation conditions[20]. Approximately 10 nm TiO_2 nanoparticles prepared by sol-gel method gradually transition from anatase into rutile during 550–650°C annealing[21]. The transformation of TiO_2 particles around 200 nm in diameter occurs in

the range of 750–850°C[22]. Curiously, 8–21 nm particles has also given a constant transition initiation temperature at 520°C[23]. To the contrary, 45 nm particles transition at relatively high temperature 900–1200°C when prepared by metalorganic chemical vapor deposition (MOCVD) at 700°C[20]. Generally, reactions at high temperatures tend to consume unreacted precursors and accelerate crystallization from the amorphous phase. Thus, one of the possible reasons for this mismatch would be that sol-gel samples may contain the tiny particles or unreacted precursors. Based on equation (1), since small particles have a low transition initiation temperature, we may have misconceived the transition of the smallest-size contamination at the low temperature as the transition initiation for the sample during the heating measurement; and besides, it is difficult to detect small-size contaminants. X-ray diffraction (XRD) gives strong evidence for existence of crystalline materials with sharp refraction peaks but not for absence of amorphous and small-size contaminants that show broad and unclear peaks. Similarly, these small contaminations give undetectable foggy images in transmission electron microscopy (TEM) when we focus on the mean-size particles, especially for light-element materials like TiO_2. The undetectable contaminants can mislead the discussions for the size dependence based on the mean size. On the other hand, some theoretical simulations predict that the anatase phase is conversely more stable than the rutile phase for nanocrystals less than 14 nm in size[24–27], Because these simulations are based on thermodynamics, the simulations basically assume that phase equilibrium exists between anatase and rutile for various crystal shapes and surface passivation to discuss phase stability and phase transition in the nano scale. If the assumption were true, the rutile phase formed by the thermal transition would return into the anatase phase at room temperature. To challenge the well-accepted experiments and theoretical calculations, we design a new experimental system using quantum size (Q-size) TiO_2 prepared from restricted numbers of titanium ions within dendrimer templates and optical wave guide (OWG) spectroscopy[28] because the atomic-level precision in size is appropriate to examine the size dependence of nano phenomena and the bandgap energy observed with OWG spectroscopy is sensitive to the size and crystal phase in the crystal-nucleus-scale[29]. In this paper, we identify whether the irreversible anatase-rutile phase transition exists in the crystal-nucleus scale or not by the size dependence in transition initiation temperature using a multi-data set instead of the conventional analyses incompetent in the crystal-nucleus-scale.

Since phenylazomethine dendrimer (DPA) used in the following experiments can control the number of metal ions in the metal assembly process, it acts as a template to provide atomic-level precise Q-size TiO_2[29]. Dendrimer has attracted much attention as a template for nanoparticles because of the well-defined size with a single molecular weight as a branched polymer synthesized through the perfectly-regulated architecture[30–32]. As a distinguished feature of DPA, metal chlorides coordinate with phenylazomethine units within DPA in a radial stepwise manner reflecting the layer-by-layer gradient in basicity of phenylazomethine units[29,33]. Thus, DPA template assembles 14 and 30 equivalents of $Ti(acac)Cl_3$, where acac is acetylacetonate, to produce the number-corresponding Q-size TiO_2 ($14TiO_2$ and $30TiO_2$) ca. 1.3 and 1.6 nm on substrate, respectively; the restriction of the component number also results in the small standard deviation (s.d.), 0.2 nm. These advantages in size control are suitable to discuss the size dependence for particles less than 2 nm. In the previous paper, the authors reported the size dependence in bandgap energy observed with OWG spectroscopy. The size dependence is practically described as follows:

$$E(r) \approx E_{\text{bulk}} + \frac{\hbar^2 \pi^2}{2r^2} \frac{1}{\mu'} - \frac{1.8e^2}{\varepsilon r} \qquad (2)$$

where $E(r)$ is size-dependent bandgap energy; $\hbar$ is Planck's constant; e is the charge on the electron; E_{bulk} is the bandgap in the bulk; μ' is the *semi-empirically adjusted* reduced mass; and ε is the dielectric constant of the bulk semiconductor (see; the further explanation in Supplementary Fig. S1). The different chemical conversion procedures using hydrolysis and thermolysis provide the same size particles, but different $E(r)$. Equation (2) explains that $E(r)$ strictly senses the size of Q-size TiO_2 and the difference in crystal structure. Recently, these results have been supported by first-principles simulations[34–36]. The sensibility is beneficial to detect the crystal-nucleus-scale phenomena after the thermal treatment. Note that Q-size TiO_2 is sintered in air at 500°C for 1 hour to remove the dendrimer templates, which is sufficient time to crystallize Q-size TiO_2 and consume the unreacted precursors in the templates. To strengthen the correlation with other studies, herein, we first prepared 2 nm Q-size TiO_2 using tetraphenylmethane core dendrimer (TPM-DPA) template; TPM-DPA is the biggest derivative in DPAs[37], which has 60 binding sites for metal ions to form $60TiO_2$ ca. 2 nm in size. The 60 equiv. of $Ti(acac)Cl_3$ within TPM-DPA transform into $60TiO_2$ on substrate using the previously reported procedure as well as $14TiO_2$ and $30TiO_2$, and then we observed size-dependent and irreversible phase transition of the anatase Q-size TiO_2 accompanied with the size growth (Fig. 1)[29]. The results support our hypothesis and suggest that Q-size TiO_2 maintains some parts of the bulk crystal structure even less than 2 nm in size.

Results

The assembling process of $Ti(acac)Cl_3$ into TPM-DPA is confirmed by the previously established procedures (Supplementary Fig. S2)[29,33,37–39], particularly the observation of isosbestic points in UV-vis absorption spectra: observing iso-points including isosbestic points is a strong tool to distinguish stepwise processes in complex systems[40]. The isosbestic points observed in UV-vis absorption spectra indicate the radial stepwise coordination of $Ti(acac)Cl_3$ within TPM-DPA until an addition of a stoichiometric amount (per imine site) of $Ti(acac)Cl_3$. Since $Ti(acac)Cl_3$ has an absorption around 300–400 nm at which DPA derivatives show the isosbestic points during the coordination, we can subtract the absorption for the added $Ti(acac)Cl_3$ from all figures to clarify the stoichiometry with the isosbestic points. After this subtraction, the isosbestic points appear

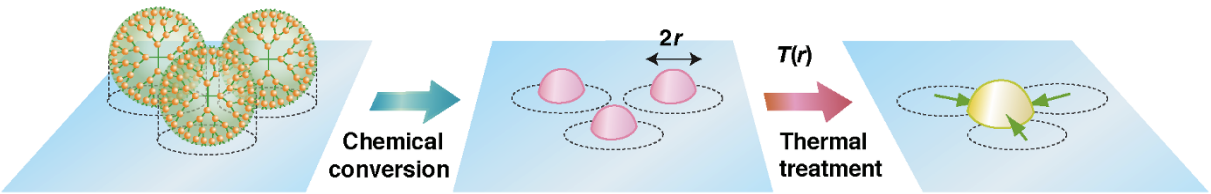

Figure 1 | Schismatic protocol for preparation and thermal treatment of Q-size TiO_2. To prevent molecular aggregation, we control the cast amount of the dendrimer templates assembling $Ti(acac)Cl_3$ based on the molecular size and spread the solution on substrates. Thus, the size of the dendrimer templates determines the maximum dot density, ca. 10^{13} cm^{-2}. The chemical conversions using hydrolysis and thermolysis provide rutile and anatase crystal phases, respectively. At the final process, combination of annealing at 500°C and UV-O_3 cleaning eliminates the dendrimer template. The thermal treatment for the anatase Q-size TiO_2 reveals that anatase phase irreversibly transforms into rutile phase at $T(r)$ through the melting-like process.

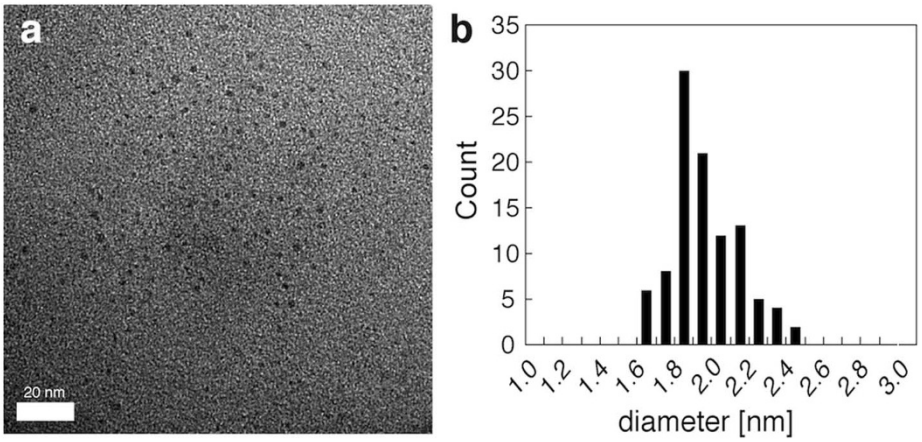

Figure 2 | TEM analysis of 60TiO$_2$. (a) TEM image and (b) the size distribution of 60TiO$_2$. The TEM sample was prepared without annealing at 500°C due to no heat resistant TEM grids.

to identify four distinct transitions: 363 nm for 0–4 equiv.; 358 nm for 5–12 equiv.; 354 nm for 14–28 equiv.; and 351 nm for 32–60 equiv., indicating that the coordination proceeds in a stepwise manner. The existence of an isosbestic point reveals the quantitative transformation of the compound; thus, the observation of the four distinct isosbestic points indicates the successive four different coordination processes upon the Ti(acac)Cl$_3$ addition. The number of added equivalents of Ti(acac)Cl$_3$ at each transition agrees with that of the binding sites present in the different layers programmed in TPM-DPA. These results are consistent with those in the case of titration of Ti(acac)Cl$_3$ into DPA[29]. The titration results indicate that the coordination also proceeds in a stepwise fashion from the core to the terminal imines of TPM-DPA.

Figure 2 shows a TEM image of hydrolysed 60TiO$_2$ and Table 1 summarizes the other size characteristic data for 60TiO$_2$. The diameter of the particle observed in TEM is 1.97 ± 0.15 (s.d., n = 100) nm, which agrees with the modelling sizes cleaved from the bulk crystal structures (Supplementary Fig. S3). The AFM images of the hydrolysed and thermorised 60TiO$_2$ reveal that the chemical conversion process does not affect the heights (Supplementary Fig. S4). As observed in 14 and 30TiO$_2$, $E(r)$ estimated from the Tauc plot of OWG spectra depends on the chemical conversion process (Supplementary Fig. S5). The experimental $E(r)$ of hydrolysed and thermorised 60TiO$_2$ corresponds with $E(r)$ calculated using equation (2) for the rutile and anatase parameters, respectively (Supplementary Fig. S6). These results indicate that the TPM-DPA serves as a template for precise size control of size of 60TiO$_2$ and that rutile phase as well as anatase phase forms in nano scale less than 2 nm.

To monitor thermal effect on the anatase Q-size TiO$_2$, we applied OWG spectra because $E(r)$ of TiO$_2$ senses the structural changes in the range of 1–5 nm; larger and rutile particles have smaller bandgap, showing a longer absorption tail. The OWG spectra obtained after annealing at each temperature for 1 hour and cooling to room temperature reveal that $E(r)$ sharply drop within 50°C at size dependent temperature. The experimental system figures that 14, 30 and 60TiO$_2$ grow from 1.3, 1.6, and 2.0 nm to 2.8, 3.6, and 4.9 nm after the anatase-rutile phase transitions at 600, 650, and 750°C, respectively (Fig. 3). All observed $E(r)$ is less than 3.2 eV, which is an evidence of the irreversible phase transition from anatase to rutile. According to the cleaved models for these size particles, the sizes estimated from the dropped $E(r)$ agree with sizes after three of each dot merges. Since the OWG spectra are observed after cooling to room temperature, the observations reveal that the rutile phase irreversibly occurs without returning to the anatase phase even though the size of the grown particles is less than 5 nm.

Table 1 | Characteristics of 60TiO$_2$

	Hydrolysis	Thermolysis
Modelling (nm)[a]	1.83	1.92
AFM (height, nm)[b]	1.31 ± 0.21	1.38 ± 0.17
$E(r)$ (eV)[c]	3.24	3.34
$2r$ (nm)[d]	1.84	1.97

[a]Assuming the spherical growth of the bulk crystal structure of the rutile and anatase forms (Supplementary Fig. S3).
[b]AFM images are shown in Supplementary Fig. S4. Error bar denotes s.d. (n = 30).
[c]Estimated from the Tauc plots of the OWG spectra (Supplementary Fig. S5).
[d]Calculated from $E(r)$ using equation (2).

Discussion

These results support the hypothesis that the irreversible phase transition occurs after the melting-like process of the anatase structure. Since Q-size TiO$_2$ binds with the substrate strongly enough to resist a mechanical wipe with methanol, the solid Q-size TiO$_2$ is likely to grow in size with the melting-like process for diffusion on the substrate during the thermal treatment at $T(r)$. Considering the cast amount of the Ti-assembling dendrimer templates and both sizes of the templates as well as formed Q-size TiO$_2$, the diffusion distances of Q-size TiO$_2$ are estimated to be ca. 1 nm, a reasonable distance for the diffusion during 1-hr thermal treatment based on the diffusion constant[41]. Furthermore, the transition initiation

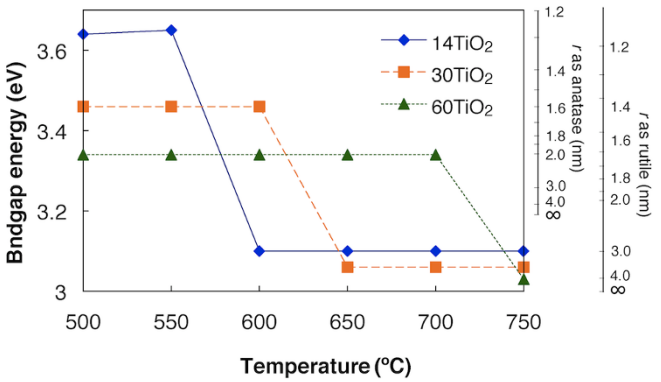

Figure 3 | Thermal bandgap shift of 14, 30, and 60TiO$_2$ observed in OWG spectra. Since equation (2) correlates the size and bandgap of anatase and rutile, the OWG spectroscopy reveals that the phase transits from anatase to rutile irreversibly, size dependently, and accompanied with the size growth through the melting-like process.

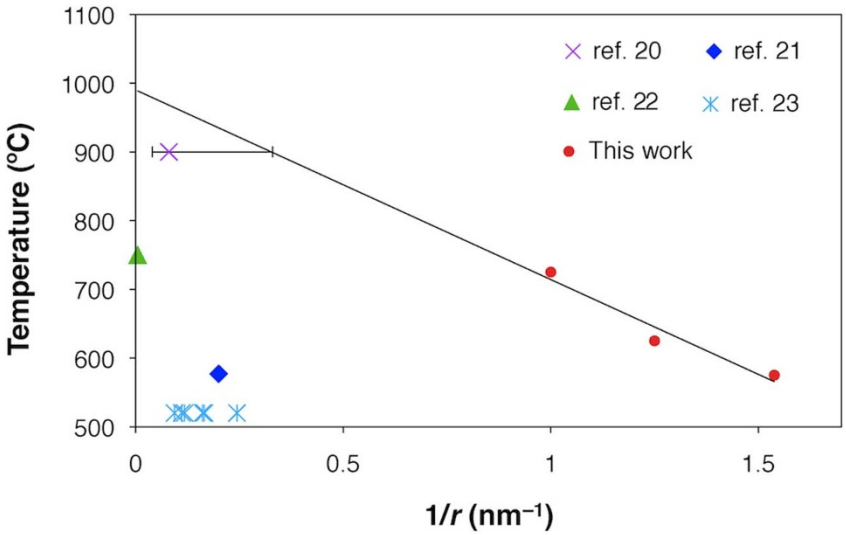

Figure 4 | Size dependence in the transition initiation temperature from anatase to rutile. Error bar for ref. 20 denotes the size distribution observed in the TEM image. The regression line gives $T_{bulk} = 990$ and $A = 276$. The coefficient of determination is 95%. The obtained T_{bulk} strongly agrees with the reported T_{bulk}.

temperature decreases with $1/r$, as predicted by equation (1) (Fig. 4). The intercept, T_{bulk}, is 990°C, which is comparable to T_{bulk} reported for pure bulk TiO_2, ca. 1000°C[18,19]. Additionally, the size dependence agrees with the plot for the smallest particles in the MOCVD sample; the transformation initiation temperature for the MOCVD sample corresponds to the transformation initiation of the smallest particles in the sample. These strong agreements in the intercept and slop support that the observed size dependence would correlate with the physical parameters for the thermal phase transition from anatase to rutile through the melting-like process.

Contrary to the theoretical predictions of the phase stability based on thermodynamics, the irreversible thermal phase transition gives the rutile phase less than 5 nm through the melting-like process. As equation (1) indicates that large-size dot has higher transition initiation temperature, the grown dots cannot maintain the melting-like state and then result in solidification. As mentioned above, the observation of $E(r)$ less than 3.2 eV after the phase transition and the size dependence of $T(r)$ corresponding to T_{bulk} and $T(r)$ for the MOCVD sample indicates that the rutile phase irreversibly forms from the anatase phase during the solidification. The thermal stability observed in $E(r)$ after the phase transition also agrees with the formation of rutile phase. Since the melting temperature of rutile phase is ca. 1840°C and remarkably higher than the phase transition temperature of anatase in bulk, it is difficult to observe the further size growth caused by melting of the rutile phase in the thermal range for this experimental setup. Moreover, the anatase-rutile transformation is also confirmed by the reasonable shift in binding energy for Ti2p observed with X-ray photoelectron spectroscopy (XPS), which is a strong tool to identify Q-size TiO_2 (Supplementary Fig. S7)[29]. The rutile formation suggests that we cannot discuss the phase stability for the irreversible transitions from the metastable anatase phase to the thermal stable rutile phase based on the thermodynamic simulations of the nano structure, surface stabilization, or phase diagram. If thermodynamic energy were the only factor to determine the stability of states, no metastable states would exist in the world.

Metastable states kinetically develop in the crystal growth reactions without reaching the stable state at each reaction step when the chemical bonds are too strong to free from the metastable states to the stable states. From this perspective, the phase of TiO_2 depends on which of the phases grows faster during polymerization of TiO_6 octahedral units as the crystal nucleation (Fig. 5). Some have already reported that anions and solvents affect the phase and shape of TiO_2 nanoparticles obtained from crystal growth in solution due to the adsorption on reaction sites to inhabit growth of certain crystal structures or crystal faces[42–45]. As the first step of the crystal growth, tiny crystal nuclei for each crystal structure will form depending on the environmental factors. The difference in the crystal structure originates from order of TiO_6 octahedral units; zigzag packing for anatase and linear packing for rutile. The zigzag packing uses only the *cis*-coordination sites of the octahedra for the crystal growth, but the linear packing requires the *trans*-coordination sites bridging two octahedra too. Although the linear packing results in the thermal stable structure due to the closest packing of TiO_6 octahedral units, the bridging structure is unstable under the kinetic control condition. Once the metastable anatase forms, it cannot transform to rutile without melting-like process at $T(r)$ because Ti-O bonds have strong binding energy as an ionic covalent bond.

The kinetic and thermodynamic control nucleation model also explains the fact that the crystal phase of Q-size TiO_2 depends on the different chemical conversion processes, simply because we can consider Q-size TiO_2 as the crystal-nucleus-size TiO_2. In the other words, since the number of titanium ions in the dendrimer templates inhibits the further crystal growth after the formation of the crystal-nucleus-size TiO_2 with size precision, the dendrimer templates allow us to study the crystal nucleation process. These results are the first evidence that the crystal nuclei have the phase difference[29], although it has been believed that the difference would diverge crystal phase in nanocrystals because the crystal growth reactions continuously occur on the surfaces of the crystal nuclei. Considering that the ionic covalent bond maintains the metastable structure in nano scale, we can also conclude that the atomic-level precision of quantum-size TiO_2 would originate from the strong binding energy of Ti-O ionic covalent bonds. The nucleation model explains how the phase difference forms; still, it is unclear how the difference in the chemical conversion processes accelerates which of the kinetic or thermodynamic control nucleation. As the future works, although the importance of kinetics in nanocrystal growth has been discussed for the size distribution and shape control[46–49], the simulation and correlating experiments to understand the factors for kinetic and thermodynamic control nucleation will be requirement to control the phase formation of nanocrystals, because of the complexity. The nucleation reactions are a complex system to give different crystal phases based on difference in the first reaction setup through multiple interactions[40]; for example, in a chemical system to synthesize nano-size TiO_2, the

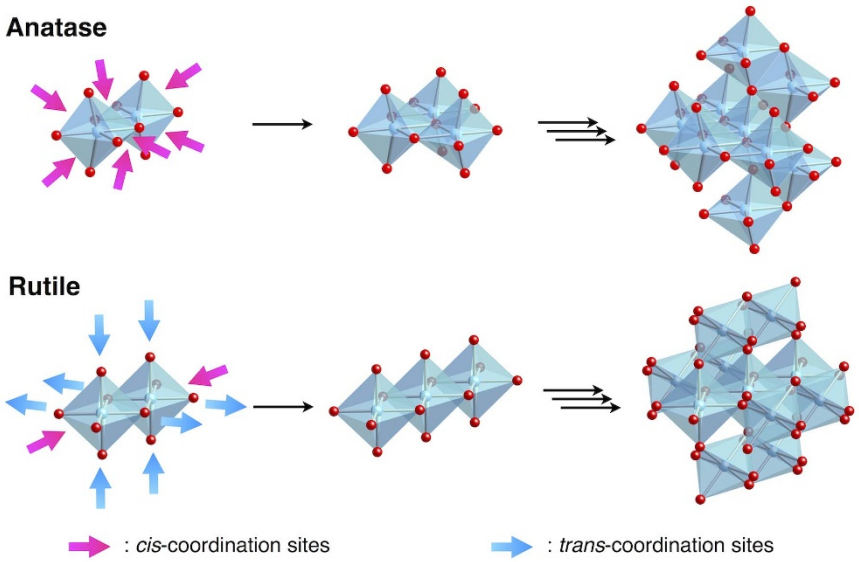

Figure 5 | Schematic image for the kinetic and thermodynamic control polymerization of TiO_6 octahedral units as the nucleation of anatase and rutile in TiO_2. Geometrically, the ratio of the *cis*-coordination sites for anatase to for rutile is 7 : 1 in the octahedral dimer. Since the symmetry is broken at the anatase trimer, only half of the *cis*-coordination sites are arrowed on the anatase dimer. The high probability for the *cis*-coordination polymerization is the reason why atanase tends to form easily as the metastable structure.

nucleation correlates with strengthen in dehydration defined by the reaction condition and with multiple interactions between TiO_6 octahedral units, ligands of Ti precursors, anions, solvents, and/or additives.

In conclusion, we have demonstrated the size dependence of the irreversible anatase-rutile phase transition in TiO_2 using the dendrimer templates for the atomic-level size control of Q-size TiO_2 and OWG spectroscopy for the detection sensitive to the crystal-nucleus-scale changes. As a result of the combination with OWG spectroscopy, the dendrimer templates give access to crystal nucleation chemistry. The sol-gel samples contain the unreacted precursors and small-size contaminants, which cannot be detected with the conventional analyses, such as XRD and TEM. These obstacles had blinded us to the size dependent phase transition and misdirected the theoretical model to discuss the phase stability. The size dependence observed in the transition initiation temperature and rutile phase formed with the size growth supports the hypothesis that the anatase phase irreversibly transits to the rutile phase through the melting-like process. To explain the metastability of anatase and the phase difference in the crystal-nucleus-size titania, we have proposed a kinetic control nucleation model from a combinational viewpoint of polymer chemistry and coordination chemistry instead of thermodynamics. The basic understanding of the thermal properties contributes to improving the energy conversion efficiency of DSCs by 10% through the thermal annealing process of TiO_2 nanocrystalline film for better connection between nanocrystals without the phase change and size growth, as recently reported[50]. Since the phase control is important for nano materials and devices, we still need the further works to understand and control the crystal phase of nanocrystals. It will probably result in direct phase control during the synthesis of nanocrystals consisting of strong chemical bonds. In addition, the paper suggests that ionic covalent bond of oxide is beneficial to construct nanostructure in atomic-level precision due to the strong binding energy, even if the nanostructure is thermodynamically unstable. Owing to the atomic-level precision, Q-size TiO_2 shows the clear size dependences in both of optical and thermal measurements for the same samples, although these measurements easily detect large-size and small-size contaminants, respectively. The concepts will contribute to the creation of artificial metastable nanostructures that we have not achieved yet with atomic-level precision.

Methods

Materials. TPM-DPA G4 was prepared according to a previous method[51]. $Ti(acac)Cl_3$ was synthesized following a literature method[52]. Q-size TiO_2 were obtained using the previous method[29]. All other chemicals were purchased from Kantoh Kagaku Co. and used as received.

Measurements. UV-vis spectra were recorded using a Shimadzu UV-3100PC spectrometer with a closed quartz cell (optical path length: 1 cm). AFM was performed using a SII SPA400 instrument under ambient conditions with the tapping mode of imaging (DFM). Si cantilevers having a spring constant of 42 N/m (SII SI-DF40P for DFM) were used at a resonance frequency of 300 kHz. A 20-μm scanner (SPA400-PZT (FS-20A), 970P3202) was used. The TEM images were obtained at 120 kV with a JEOL JEM-2010 instrument. The OWG spectra were obtained using a System Instruments Co., Ltd., SIS-5000 spectrophotometer. The XPS spectra were measured using a JEOL JPS-9000MC photoelectron spectrometer without the plasma etching process. The binding energy calibration is based on the measurement of the mica O(1s) signal, E_b = 531.61 eV[53].

1. Tolbert, S. H. & Alivisatos, A. P. Size dependence of a first order solid-solid phase transition: the wurtzite to rock salt transformation in CdSe nanocrystals. *Science* **265**, 373–376 (1994).
2. Jacobs, K., Zaziski, D., Scher, E. C., Herhold, A. B. & Alivisatos, A. P. Activation volumes for solid-solid transformations in nanocrystals. *Science* **293**, 1803–1806 (2001).
3. Rivest, J. B., Fong, L.-K., Jain, P. K., Toney, M. F. & Alivisatos, A. P. Size dependence of a temperature-induced solid–solid phase transition in copper(I) sulfide. *J. Phys. Chem. Lett.* **2**, 2402–2406 (2011).
4. Li, Y., Qi, W., Li, Y., Janssens, E. & Huang, B. Modeling the size-dependent solid–solid phase transition temperature of Cu_2S nanosolids. *J. Phys. Chem. C* **116**, 9800–9804 (2012).
5. Szwarcman, D., Vestler, D. & Markovich, G. The size-dependent ferroelectric phase transition in $BaTiO_3$ nanocrystals probed by surface plasmons. *ACS Nano* **5**, 507–515 (2011).
6. Takahashi, Y. K., Ohkubo, T., Ohnuma, M. & Hono, K. Size effect on the ordering of FePt granular films. *J. Appl. Phys.* **93**, 7166 (2003).
7. Abdala, P. M., Craievich, A. F. & Lamas, D. G. Size-dependent phase transitions in nanostructured zirconia–scandia solid solutions. *RSC Advances* **2**, 5205–5213 (2012).
8. Buffat, P. & Borel, J.-P. Size effect on the melting temperature of gold particles. *Phys. Rev. A* **13**, 2287–2298 (1976).
9. Goldstein, A. N., Echer, C. M. & Alivisatos, A. P. Melting in semiconductor nanocrystals. *Science* **256**, 1425–1427 (1992).
10. Cleveland, C. L., Luedtke, W. D. & Landman, U. Melting of gold clusters: icosahedral precursors. *Phys. Rev. Lett.* **81**, 2036–2039 (1998).
11. Cleveland, C. L., Luedtke, W. D. & Landman, U. Melting of gold clusters. *Phys. Rev. B* **60**, 5065–5077 (1999).
12. Olson, E. A., Yu, M., Zhang, E. M., Zhang, Z. & Allen, L. H. Size-dependent melting of Bi nanoparticles. *J. Appl. Phys.* **97**, 034304 (2005).

13. Dick, K., Dhanasekaran, T., Zhang, Z. & Meisel, D. Size-dependent melting of silica-encapsulated gold nanoparticles. *J. Am. Chem. Soc.* **124**, 2313–2317 (2002).
14. Fujishima, A. & Honda, K. Electrochemical photolysis of water at a semiconductor electrode. *Nature* **238**, 37–38 (1972).
15. O'Regan, B. & Grätzel, M. A low-cost, high-efficiency solar cell based on dye-sensitized colloidal TiO_2 films. *Nature* **353**, 737–740 (1991).
16. Kim, J. Y. *et al*. Efficient tandem polymer solar cells fabricated by all-solution processing. *Science* **13**, 222–225 (2007).
17. Gennari, F. C. & Pasquevich, D. M. Kinetics of the anatase–rutile transformation in TiO_2 in the presence of Fe_2O_3. *J. Mater. Sci.* **33**, 1571–1578 (1998).
18. Shannon, R. D. Phase transformation studies in TiO_2 supporting different defect mechanisms in vacuum-reduced and hydrogen-reduced Rutile. *J. Appl. Phys.* **35**, 3414–3416 (1964).
19. Gamboa, J. A. & Pasquevich, D. M. Effect of additives on photocatalytic activity of titanium dioxide powders synthesized by thermal plasma. *J. Am. Ceram. Soc.* **75**, 2934–2938 (1992).
20. Sun, Y., Egawa, T., Zhang, L. & Yao, X. High anatase-rutile transformation temperature of anatase titania nanoparticles prepared by metalorganic chemical vapor deposition. *Jpn. J. Appl. Phys.* **41**, L 945–L 948 (2002).
21. Zhang, H. & Banfield, J. F. Understanding polymorphic phase transformation behavior during growth of nanocrystalline aggregates: insights from TiO2. *J. Phys. Chem. B* **104**, 3481–3487 (2000).
22. Pal, M., Serrano, J. G., Santiago, P. & Pal, U. Size-controlled synthesis of spherical TiO_2 nanoparticles: morphology, crystallization, and phase transition. *J. Phys. Chem. C* **111**, 96–102 (2007).
23. Zhang, H. & Banfield, J. F. Size dependence of the kinetic rate constant for phase transformation in TiO_2 nanoparticles. *Chem. Mater.* **17**, 3421–3425 (2005).
24. Lu, H. M., Zhang, W. X. & Jiang, Q. Phase Stability of Nanoanatase. *Adv. Eng. Mater.* **5**, 787–788 (2003).
25. Barnard, A. S. & Curtiss, L. A. Prediction of TiO_2 nanoparticle phase and shape transitions controlled by surface chemistry. *Nano Lett.* **5**, 1261–1266 (2005).
26. Guisbiers, G., Van Overschelde, O. & Wautelet, M. Theoretical investigation of size and shape effects on the melting temperature and energy bandgap of TiO_2 nanostructures. *Appl. Phys. Lett.* **92**, 103121 (2008).
27. Barnard, A. S. & Xu, H. An environmentally sensitive phase map of titania nanocrystals. *ACS Nano* **2**, 2237–2242 (2008).
28. Takahashi, H., Fujita, K. & Ohno, H. Direct visible spectral analysis of solid samples by optical waveguide spectroscopy due to adsorbed sample molecules after sublimation. *Chem. Lett.* **36**, 116–117 (2007).
29. Satoh, N., Nakashima, T., Kamikura, K. & Yamamoto, K. Quantum size effect in TiO_2 nanoparticles prepared by finely controlled metal assembly on dendrimer templates. *Nature. Nanotech.* **3**, 106–111 (2008).
30. Tomalia, D. A. Dendrons/dendrimers: quantized, nano-element like building blocks for soft-soft and soft-hard nano-compound synthesis. *Soft Matter.* **6**, 456–474 (2010).
31. Astruc, D., Boisselier, E. & Ornelas, C. Dendrimers designed for functions: from physical, photophysical, and supramolecular properties to applications in sensing, catalysis, molecular electronics, photonics, and nanomedicine. *Chem. Rev.* **110**, 1857–1959 (2010).
32. Myers, V. S. *et al.* Dendrimer-encapsulated nanoparticles: New synthetic and characterization methods and catalytic applications. *Chem. Sci.* **2**, 1632–1646 (2011).
33. Yamamoto, K., Higuchi, M., Shiki, S., Tsuruta, M. & Chiba, H. Stepwise radial complexation of imine groups in phenylazomethine dendrimers. *Nature* **415**, 509–511 (2002).
34. Peng, H., Li, J., Li, S.-S. & Xia, J.-B. First-principles study on rutile TiO_2 quantum dots. *J. Phys. Chem. C* **112**, 13964–13969 (2008).
35. Iacomino, A., Cantele, G., Ninno, D., Marri, I. & Ossicini, S. Structural, electronic, and surface properties of anatase TiO_2 nanocrystals from first principles. *Phys. Rev. B* **78**, 075405 (2008).
36. Sahoo, S. K., Pal, S., Sarkar, P. & Majumder, C. Size-dependent electronic structure of rutile TiO_2 quantum dots. *Chem. Phys. Lett.* **516**, 68–71 (2011).
37. Yamamoto, K. *et al.* Size-specific catalytic activity of platinum clusters enhances oxygen reduction reactions. *Nature Chem.* **1**, 397–402 (2009).
38. Satoh, N., Nakashima, T. & Yamamoto, K. Metal-assembling dendrimers with a triarylamine core and their application to a dye-sensitized solar cell. *J. Am. Chem. Soc.* **127**, 13030–13038 (2005).
39. Satoh, N. & Yamamoto, K. Self-assembled monolayers of metal-assembling dendron thiolate formed from dendrimers with a disulfide core. *Org. Lett.* **11**, 1729–1732 (2009).
40. Satoh, N. & Han, L. Chemical input and I–V output: stepwise chemical information processing in dye-sensitized solar cells. *Phys. Chem. Chem. Phys.* **14**, 16014–16022 (2012).
41. Hoshino, K., Peterson, N. L. & Wiley, C. L. Diffusion and point-defects in TiO2-X. *J. Phys. Chem. Solid.* **46**, 1397–1411 (1985).
42. Jun, Y.-W. *et al.* Surfactant-assisted elimination of a high energy facet as a means of controlling the shapes of TiO_2 nanocrystals. *J. Am. Chem. Soc.* **125**, 15981–15985 (2003).
43. Yan, M., Chen, F., Zhang, J. & Anpo, M. Preparation of controllable crystalline titania and study on the photocatalytic properties. *J. Phys. Chem. B* **109**, 8673–8678 (2005).
44. Yang, H. G. *et al.* Anatase TiO_2 single crystals with a large percentage of reactive facets. *Nature* **453**, 638–641 (2008).
45. Yang, H. G. *et al.* Solvothermal synthesis and photoreactivity of anatase TiO_2 nanosheets with dominant {001} facets. *J. Am. Chem. Soc.* **131**, 4078–4083 (2009).
46. Peng, X., Wickham, J. & Alivisatos, A. P. Kinetics of II-VI and III-V colloidal semiconductor nanocrystal growth: "focusing" of size distributions. *J. Am. Chem. Soc.* **120**, 5343–5344 (1998).
47. Manna, L., Scher, E. C. & Alivisatos, A. P. Synthesis of soluble and processable rod-, arrow-, teardrop-, and tetrapod-shaped CdSe nanocrystals. *J. Am. Chem. Soc.* **122**, 12700–12706 (2000).
48. Jun, Y.-W., Choi, J.-S. & Cheon, J. Shape control of semiconductor and metal oxide nanocrystals through nonhydrolytic colloidal routes. *Angew. Chem. Int. Ed.* **45**, 3414–3439 (2006).
49. Yu, Y., Zhang, Q., Xie, J. & Lee, J. Y. Engineering the architectural diversity of heterogeneous metallic nanocrystals. *Nat. Commu.* **4**, 1454 (2013).
50. Fabbri, F. *et al.* Thermal processing and characterizations of dye-sensitized solar cells based on nanostructured TiO2. *J. Phys. Chem. C* **117**, 3729–3738 (2013).
51. Enoki, O., Katoh, H. & Yamamoto, K. Synthesis and properties of a novel phenylazomethine dendrimer with a tetraphenylmethane core. *Org. Lett.* **8**, 569–571 (2006).
52. Serpone, N., Bird, P. H., Somogyvari, A. & Bickley, D. G. Five-coordinate titanium(IV) complexes. Infrared spectral studies on X_3Ti(diketonato) and XY_2Ti(diketonato) complexes and the crystal and molecular structure of di-.μ.-chloro-tetrachlorobis(2,4-pentanedionato)dititanium(IV). *Inorg. Chem.* **16**, 2381–2386 (1977).
53. Liu, Z. H. & Brown, N. M. D. XPS characterization of mica surfaces processed using a radio-frequency (rf) argon plasma. *J. Phys. D, Appl. Phys.* **31**, 1771 (1998).

Acknowledgements

This work was partially supported by CREST from the Japan Science and Technology Agency. NS acknowledges Grants-in-Aid for Scientific Research (No. 20850032 and 21750151) provided from JSPS.

Author contributions

N.S. and T.N. conceived and designed the experiments. N.S. developed the theoretical concept. N.S. and K.Y. wrote the paper. K.Y. supervised all the works.

Additional information

Supplementary information accompanies this paper at http://www.nature.com/scientificreports

Competing financial interests: The authors declare no competing financial interests.

How to cite this article: Satoh, N., Nakashima, T. & Yamamoto, K. Metastability of anatase: size dependent and irreversible anatase-rutile phase transition in atomic-level precise titania. *Sci. Rep.* **3**, 1959; DOI:10.1038/srep01959 (2013).